BIOCHEMISTRY
including biophysical chemistry & molecular biology

Article

pubs.acs.org/biochemistry

Challenges in the Interpretation of Protein H/D Exchange Data: A Molecular Dynamics Simulation Perspective

Robert G. McAllister and Lars Konermann*

Department of Chemistry, The University of Western Ontario, London, Ontario N6A 5B7, Canada

Supporting Information

ABSTRACT: Many protein structural investigations involve the use of H/D exchange (HDX) techniques. It is commonly thought that amide backbone protection arises from intramolecular H-bonding and/or burial of NH sites. Recently, fundamental HDX-related tenets have been called into question. The current work focuses on ubiquitin for exploring the defining features that distinguish amides in "open" (exchange-competent) and "closed" (exchange-incompetent) environments. Instead of relying on static X-ray structures, we employ all-atom molecular dynamics (MD) simulations for obtaining a dynamic view of the protein ground state and its surrounding solvent. The HDX properties for 57 out of 72 NH sites can be readily explained on the basis of backbone and side chain H-bonding, as well as solvent accessibility considerations. Unexpectedly, the same criteria fail for predicting the HDX characteristics of the remaining 15 amides. Significant protection is seen for numerous exposed NH sites that are not engaged in intramolecular H-bonds, whereas other amides that seemingly share the same features are unprotected. We scrutinize the proposal that H-bonding to crystallographically defined water can cause the protection of surface amides. For ubiquitin, the positioning of crystal water is not compatible with this idea. To further explore possible solvation effects, we tested for the presence of partially immobilized water networks. Our MD data reveal no difference in the solvation properties of protected vs unprotected surface amides, making it unlikely that restricted water dynamics can cause anomalous amide protection. The findings reported here suggest that efforts to deduce protein structural features on the basis of HDX protection factors may yield misleading results. This conclusion is relevant for initiatives that rely on sparse structural data as constraints for elucidating protein conformations. It may be necessary to pursue detailed quantum mechanical studies of the protein, the solvent, and the hydroxide catalyst for obtaining a comprehensive understanding of the factors that govern HDX rates. The considerable size of the systems involved makes such endeavors a daunting task.

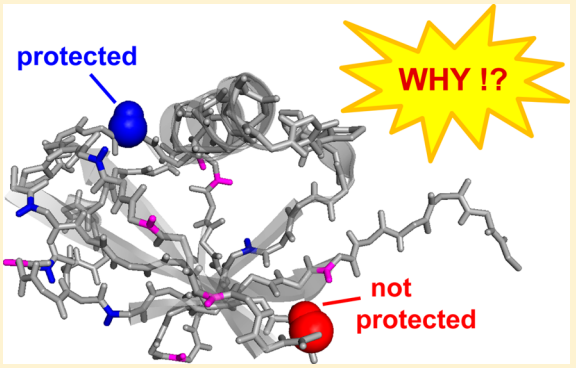

Backbone H/D exchange (HDX) measurements are widely used for studying protein structure and dynamics. Both NMR spectroscopy[1−4] and mass spectrometry[5−14] can serve as detection methods. Ideally, these measurements yield the HDX rate constant k_{HDX} for each single NH site.

In short peptides, the deuteration kinetics are governed by the two side chains adjacent to the amide of interest. HDX in near-neutral solution proceeds with OD^- catalysis through a R−C(O^-)=N−R imidate that subsequently interacts with D_2O to form R−CO−ND−R.[15] Positive charge density in the vicinity of the NH lowers the amide pK_a by stabilizing the imidate, thereby accelerating HDX. The opposite effect is encountered for negative charge.[16−18] Accordingly, the interactions between a peptide NH and its two adjacent side chains can be attributed to inductive effects, with some modulation by steric factors.[19] Empirical rules have been established to describe how these nearest neighbor interactions determine the second-order rate constant k_B, resulting in an overall peptide "chemical" rate constant[19]

$$k_{ch} = k_B \times [OD^-] \quad (1)$$

Additional considerations are required to understand HDX in proteins. Disordered segments are said to be in an "open" state, and they exchange with rates close to those expected for short peptides ($k_{HDX} \approx k_{ch}$).[19] In contrast, HDX in structured regions tends to proceed much more slowly. The factors contributing to the protection of these amides remain controversial. It is instructive to briefly highlight some of the pertinent issues.

Solvent accessibility is often quoted as an important determinant of HDX rates.[11,20−24] This notion is in sharp contrast to the view that protection is chiefly governed by H-bonding,[25] typically via backbone NH···OC contacts.[26] Experiments confirm that H-bonded amides usually exhibit strong protection, even if they are at the surface.[25] The H-bond-centric view emphasizes the role of conformational dynamics. Accordingly, NH groups in structured segments predominantly reside in a "closed" (exchange-incompetent) state, but they can

Received: February 28, 2015
Revised: April 4, 2015
Published: April 10, 2015

DOI: 10.1021/acs.biochem.5b00215
Biochemistry 2015, 54, 2683−2692

undergo transient opening events that briefly disrupt H-bonds and provide NH contact with the solvent. HDX-relevant fluctuations can range from local events all the way to global unfolding/refolding.[1] During the brief time intervals that NH sites spend in the "open" state they may undergo deuteration with the rate constant k_{ch} (eq 1). The resulting HDX mechanism can be expressed as[27]

$$\mathrm{NH_{closed}} \underset{k_{cl}}{\overset{k_{op}}{\rightleftarrows}} \mathrm{NH_{open}} \xrightarrow[\mathrm{D_2O}]{k_{ch}} \text{exchanged} \tag{2}$$

This framework yields an EX2 rate constant $k_{HDX} = (k_{op}/k_{cl})k_{ch}$. The extent of protection relative to the peptide-calibrated state can be reported as[6,25,26]

$$\log P = \log(k_{ch}/k_{HDX}) \tag{3}$$

Although the H-bond-centric view is quite well established,[2,6,25,26] the relative importance of steric shielding (without H-bonding, e.g., in collapsed regions[28]) remains an open question.

The above considerations notwithstanding, some amides exchange very slowly, despite being apparently solvent accessible and free of H-bonds.[25,29−31] This phenomenon is difficult to reconcile with traditional views of the HDX process. It has been proposed that such anomalous protection arises from tertiary interactions that provide a unique electrostatic environment, thereby affecting the NH pK_a in ways that go beyond the nearest neighbor effects seen in peptides.[19] This idea shows promise in some cases,[29,32] but fails in others.[25] A competing proposal[25,33] dismisses the importance of tertiary electrostatic contacts. Instead, it envisions that exposed NH sites can be protected by H-bonding to crystallographically defined waters at the protein surface. This alternative view re-emphasizes the role of H-bonding for HDX protection, by including tightly bound waters as suitable H-bond acceptors.[34,43] The idea of NH protection via water contacts is intriguing, but it has not been thoroughly tested yet.[32]

The inter-related issues outlined above complicate the interpretation of HDX experiments. Very basic concepts such as the exact nature of "closed" and "open" conformations remain nebulous. These difficulties may be partly rooted in the fact that HDX data are often interpreted in the context of static X-ray structures.[5,22,23,26,32,33] Crystal packing effects can significantly distort amide exposure and H-bonding.[33,34] Hence, X-ray structures may not properly represent the thermally activated ensemble encountered under ambient solution conditions. Molecular dynamics (MD) simulations[35−41] and related computational approaches[24,42,43] can help address these shortcomings by providing a dynamic view of the protein and its solvent environment. Unfortunately, the microsecond to millisecond range accessible in all-atom MD simulations[44] is much shorter than most HDX-relevant conformational fluctuations.[25] Coarse-grained simulations provide better conformational sampling[36] but lack structural details, thereby complicating comparisons with experimental data. Despite these limitations, MD data should provide a better comparison basis for the interpretation of HDX data than static X-ray structures.

Here we conduct all-atom MD simulations on ubiquitin to examine how well the solution phase behavior of this protein correlates with its HDX protection pattern. Ubiquitin is relatively small (76 residues, 72 backbone amides) with a well-defined native fold.[45] It was chosen for this work because its HDX behavior has been characterized in great detail, with log P values that span more than 6 orders of magnitude.[13,26,30,46,47] The disordered C-terminus lacks protection and thus serves as internal standard. Our MD simulations provide a dynamic view of the protein ground state in solution. These data allow us to scrutinize on an amide-by-amide basis in how far HDX protection can be attributed to H-bonding, solvent accessibility, crystallographic waters, or other factors. We find that the interpretation of HDX data in a protein conformational context is surprisingly difficult; 21% of all backbone amides exhibit log P values that are seemingly inconsistent with their structural environment. Our findings highlight severe shortcomings in the current understanding of structure−rate relationships, and they caution against a noncritical use of HDX data for deducing protein conformational features.

METHODS

MD Simulations. All-atom ubiquitin simulations in explicit water were conducted using GROMACS 4.6.5.[48,49] Like other MD studies on ubiquitin,[44] we used the 1.8 Å crystal structure 1UBQ[45] as starting point. Hydrogens were added using the PDB 2GMX routine. All titratable moieties were set to their standard charge states expected for pH 7 (N-terminus$^+$, R$^+$, K$^+$, D$^-$, E$^-$, C-terminus$^-$) with H68 in its deprotonated state, resulting in a net protein charge of zero. The discussion below will focus on data generated using the CHARMM22* force field[50] with TIP3P water.[51] In addition, simulations were conducted using Amber99sb-ILDN[52] with TIP4P water.[51] None of these (or any other commonly used) water models account for the self-dissociation of H_2O into H^+ and OH^-.[53,54] The protein was placed in a rhombic dodecahedral periodic box, with a minimum distance of 7 Å between protein atoms and the edge of the box. ∼4400 water molecules were added from a pre-equilibrated configuration file. Randomly selected solvent molecules were replaced with Na^+ or Cl^- for a total salt concentration of 150 mM. The systems were subjected to energy minimization for 800 iterations, prior to 100 ps of equilibration at 298 K and 1 bar using a velocity-rescaling thermostat[55] and Berendsen barostat.[56] Initial velocities were sampled from a Maxwell−Boltzmann distribution. One μs production runs were initialized from the equilibrated systems, using leapfrog integration with a time step of 2 fs. These simulations were carried out under NVT conditions with velocity rescaling at 298 K.[55] Bonds were constrained using the linear constraint solver algorithm for protein[57] and the SETTLE algorithm for water.[58] Short range interactions were modeled with a Lennard−Jones 10 Å potential-shifted cutoff, while electrostatics were modeled using the smooth particle-mesh Ewald method[59] with a grid spacing of 2.4 Å. The coordinates of all atoms were recorded every 2 ps for analysis.

Data Analysis. An in-house program was written in C++ to detect backbone amide H-bonds. The program reports the distance between each amide hydrogen and the closest possible H-bond acceptor (A) that satisfies the N−H-A angle criterion of 90°−180°.[60] A NH is considered to be H-bonded if the angle criterion is satisfied while at the same time the H/A distance is less than 2.5 Å (Figure 1a). All oxygen and nitrogen atoms, including those in side chains, were considered as possible A moieties. The program was designed to record the fraction of time that each NH site interacts with each possible acceptor. When discussing H-bonds between two residues we will use the

DOI: 10.1021/acs.biochem.5b00215
Biochemistry 2015, 54, 2683−2692

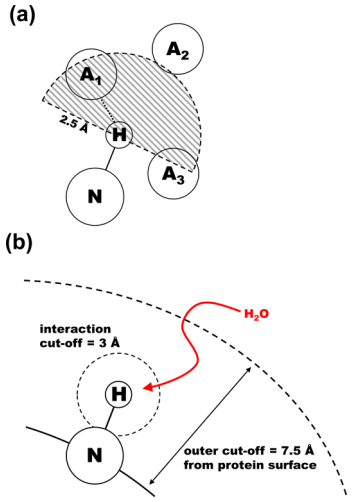

Figure 1. (a) H-bond detection algorithm. An NH is considered to be H-bonded if a possible acceptor A is located within the shaded semisphere (exemplified by A_1). A_2 is too far away; A_3 falls outside the permitted angular range. (b) Cartoon description of the algorithm used for assessing how rapidly bulk solvent can replace water molecules adjacent to a NH site ("bulk interaction rate"). One possible trajectory of a bulk H_2O (or D_2O) is indicated in red.

convention of naming the NH donor first, followed by the acceptor.

A second program was developed to measure the solvent accessible surface area (SASA) of specified atoms at each time point using the double cubic lattice method.[61] This technique models each atom as a sphere, with previously published effective van der Waals radii that represent protein interactions with water.[62] SASA values discussed below refer to the sum of the amide nitrogen and hydrogen for each residue.

To investigate the possible presence of tightly bound water networks at solvent-exposed NH sites[25,33] a "bulk interaction rate" was determined. This parameter represents a measure of how rapidly H_2O (or D_2O) molecules can diffuse from bulk solution into the direct vicinity of an NH site. For implementing this strategy, each water within 7.5 Å of the protein surface was tagged. Next, we determined how much time elapsed before the first *untagged* water came within 3 Å of the amide hydrogen (Figure 1b). This algorithm is only meaningful for NH sites that are not permanently buried. The analysis was therefore only performed for residues with greater-than-mean SASA values. The calculations were repeated 1000 times with starting points that were spaced by 1 ns. The mean of these replicates was used to determine the interaction rate in units of ps^{-1}.

RESULTS AND DISCUSSION

Ubiquitin Structure and Dynamics. All-atom MD simulations of native ubiquitin in explicit water were conducted at 298 K. During the 1 μs simulation window, the protein remained relatively close to its initial structure, with root-mean-square deviation (RMSD) values between 1 and 3 Å (Figure 2a). Global unfolding/refolding transitions were not observed. This behavior is consistent with the known high stability of ubiquitin.[45] A root-mean-square fluctuation (RMSF) plot further illustrates the rigid nature of the protein, with RMSF values of no more than 1 Å for most residues (Figure 2b). Only the C-terminal tail (residues 73−76) is more flexible, in agreement with existing structural data.[45] Local regions

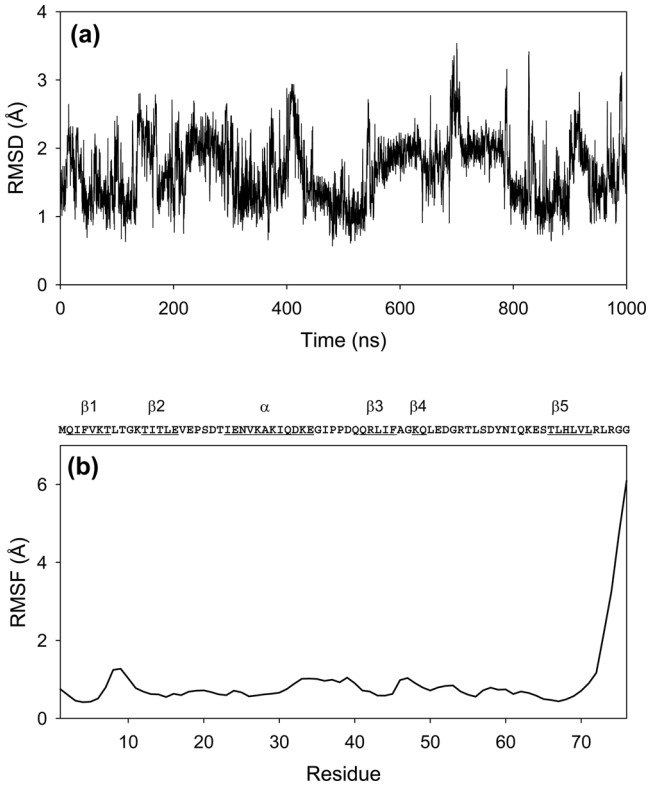

Figure 2. (a) Root-mean-square deviation of ubiquitin backbone atoms relative to the energy-minimized crystal structure. (b) Root-mean-square fluctuation of backbone atoms averaged for each residue. Panel (b) also shows the protein sequence and key secondary structure elements.

occasionally undergo opening/closing transitions, as envisioned by eq 2. For example, the H-bonds R42-L71 and R72-Q40 are intact at 944 ns (Figure 3a), whereas both contacts are broken at 946 ns (Figure 3b). A few nanoseconds later, both contacts are regenerated (not shown in Figure 3).

The H-bonding status of all backbone NH sites was tracked as a function of time. For each residue, we identified the closest possible acceptor A that satisfied the 90°−180° angle criterion, and we plotted the distance of this atom to the amide hydrogen. H/A distances below 2.5 Å imply the presence of a H-bond (Figure 1a).[60] Figure 4 exemplifies three of the profiles obtained in this way. I44 is permanently H-bonded, R72 is H-bonded most of the time, whereas G76 is almost completely free. This analysis was conducted for all NH sites, yielding average values that are summarized in Figure 5 (discussed below).

Opening/closing events of the type illustrated in Figure 3 are quite rare in our simulations. Many sites (such as I44, Figure 4a) remain permanently H-bonded on the time scale considered here, despite undergoing deuteration with finite k_{HDX} values.[13,26,30,46,47] This reflects the well-known fact that all-atom MD studies cannot adequately sample all the conformational events probed by HDX, where labeling times extend to days.[13,26,30,36,42,46,47] Even state-of-the-art (~1 ms)[44] simulations are orders of magnitude too short for this purpose.[25] Fluctuations can be enhanced by running simulations at elevated temperature,[44] but such semidenaturing conditions favor large-scale dynamics that are not adequate for modeling a native HDX environment.[1]

DOI: 10.1021/acs.biochem.5b00215
Biochemistry 2015, 54, 2683−2692

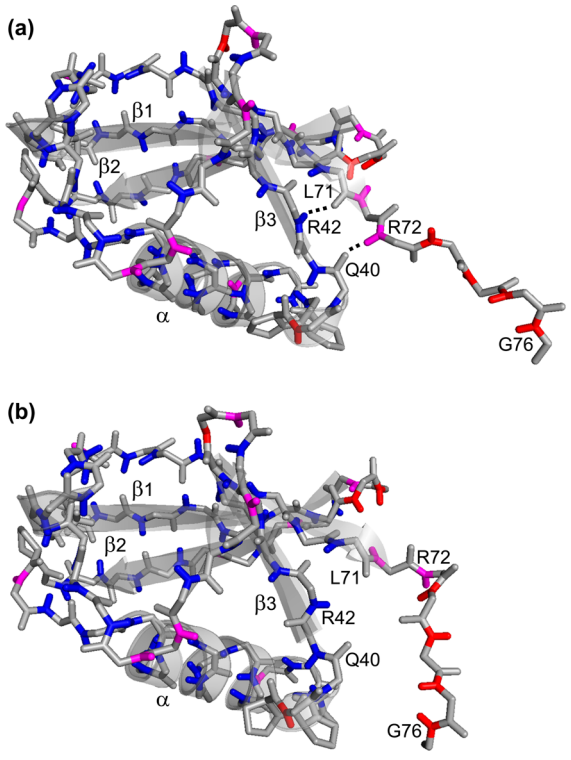

Figure 3. MD snapshots for t = 944 ns (a) and t = 946 ns (b). Side chains are omitted. Backbone NH groups are colored according to their experimental protection factors (from Figure 5a): blue, strongly protected; pink, weakly protected; red, unprotected. Panel (a) highlights two backbone H-bonds, R42-L71 and R72-Q40. In panel (b), these two H-bonds are disrupted due to a local fluctuation.

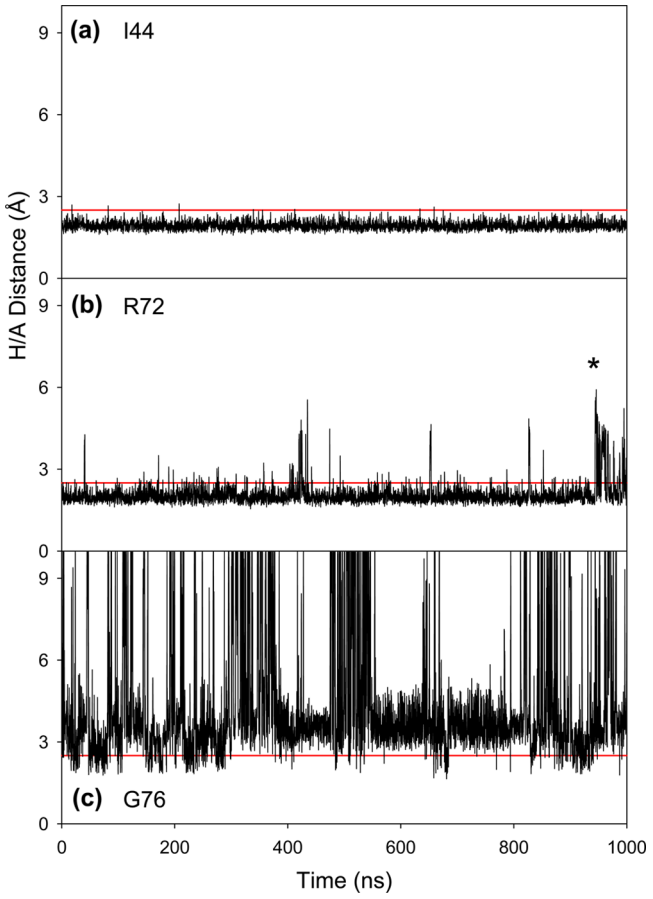

Figure 4. H-bonding properties of three NH sites. Shown is the amide hydrogen distance to the closest carbonyl acceptor ("A") that falls within the permissible angular range (see Figure 1a). H/A distances below 2.5 Å (indicated by red lines) reflect the presence of a H-bond. (a) Data for I44, with H-bonding to H68 for 100% of the time; (b) R72, with 93% H-bonding to Q40. The asterisk marks the opening event of Figure 3. (c) G76, with 7% H-bonding to L73 and 1% to D39.

In summary, although our data do not report on slow opening/closing transitions, they provide rich information on the ubiquitin ground state ensemble and its solvent environment. NH sites that are experimentally found to be protected must predominantly reside in a "closed" state under the simulation conditions used here. Conversely, sites with log $P \approx 0$ must be "open".[1,27] Our trajectories, therefore, allow a detailed examination of the structural features that cause NH sites to be "open" or "closed".

Experimental Results. Ubiquitin HDX/NMR data are available from several sources.[26,30,46,47] The log P values from different laboratories agree with each other quite well (Figure 5a), and they are also consistent with recent top-down mass spectrometry experiments.[13] Craig et al.[36] compiled an averaged log P profile that will serve as foundation for the following considerations (filled symbols in Figure 5a). To simplify the discussion we categorize amides according to their experimental behavior. NH groups with log P < 1 are considered to be *unprotected*. The remaining sites are broken down into *weakly protected* (1 < log P < 2) and *strongly protected* (log P > 2). The locations of these NH groups are highlighted in Figure 3 using red, pink, and blue, respectively.

Main Chain H-Bonds. MD simulations reveal that 42 residues are H-bonded via main chain NH···OC contacts, evident from H/A distance values that fall below the 2.5 Å threshold[60] in Figure 5b. These NH sites are highlighted green in Figure 6a. All of them fall into the strongly or weakly protected HDX/NMR categories. Many of these sites are located in the α helix and the five-stranded β sheet, consistent with the view[26] that HDX protection is often correlated with the presence of secondary structure.

Side Chain H-Bonds. In addition to main chain contacts, NH interactions with side chains are encountered (Figure 6b). Experiments show that K11, E51, and D58 are protected (Figure 5a), despite lacking H-bonds to main chain carbonyls (Figure 5b). However, inclusion of side chain atoms in our analysis lowers their H/A distance below the 2.5 Å threshold (Figure 5c). Specifically, K11 is H-bonded to the T7 side chain 83% of the time, E51 is 98% bonded to the hydroxyl group of Y59, and D58 alternates between bonding to the T55 side chain (48%) and the T55 main chain carbonyl (38%).

E18 and T55 are strongly protected, and they interact with aspartate side chains. The corresponding contacts (E18-D21 and T55-D58) fall short of the 2.5 Å distance threshold (Figure 5c). These cases represent examples of "bifurcated" H-bonds, where a backbone NH interacts with both oxygens of a carboxylate. It has been noted previously that this type of H-bond goes undetected when applying standard geometric criteria.[60] Our data nonetheless underscore the importance of bifurcated H-bonds for HDX protection.

The MD results discussed so far confirm that H-bonding generally leads to protection. Interestingly, more than 10% of the HDX-relevant H-bonds do not constitute main chain

DOI: 10.1021/acs.biochem.5b00215
Biochemistry 2015, 54, 2683−2692

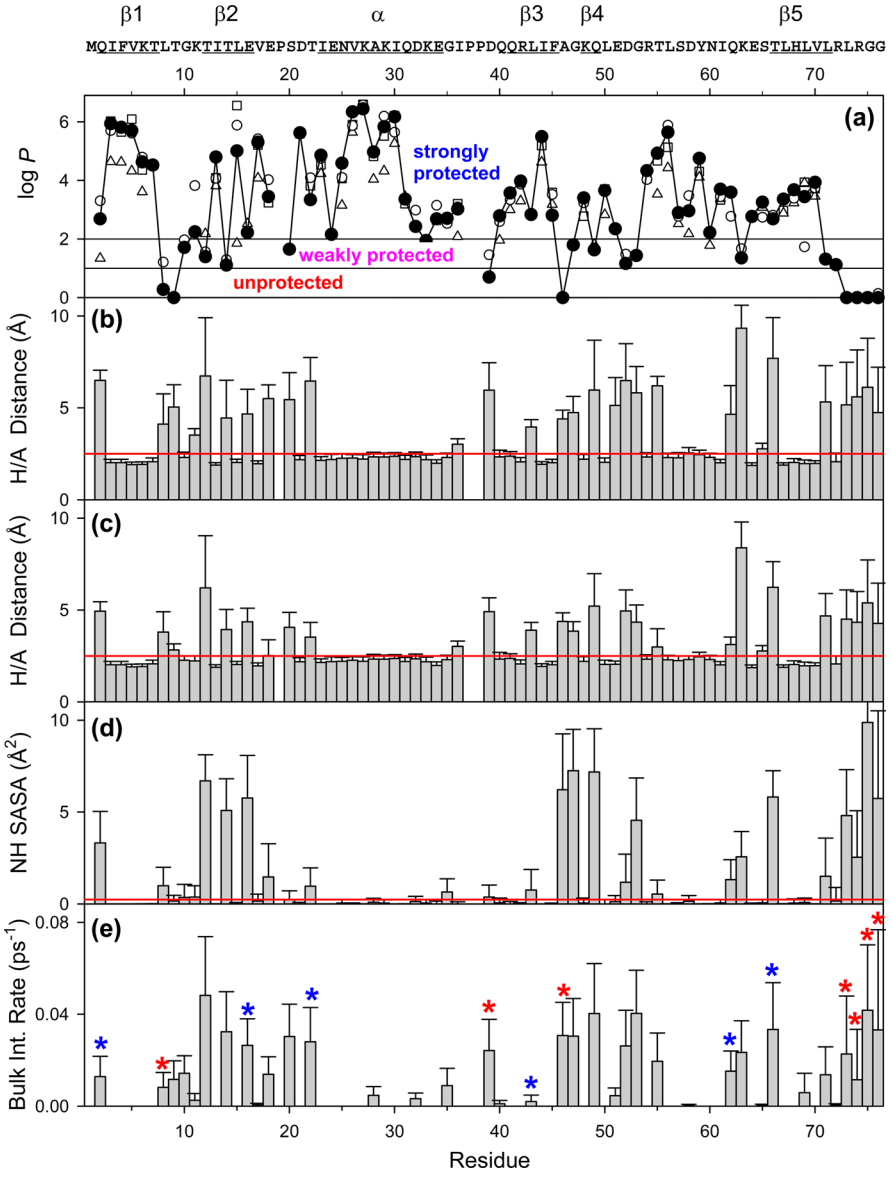

Figure 5. Overview of experimental HDX data, and various properties extracted from a 1 μs CHARMM22*/TIP3P simulation. (a) Experimental protection factors compiled by Craig et al.[36] are highlighted as solid circles. Also shown are individual data sets as open triangles,[26] open circles,[46] and open squares.[47] (b) Average distance between the backbone NH of each residue and the closest possible main chain carbonyl acceptor. Values below 2.5 Å (red line) reflect the presence of a H-bond. (c) Same as in panel (b), but including side chains. (d) Average NH SASA values. The red line represents the SASA threshold of 0.23 Å^2. (e) Average bulk interaction rate, describing how fast bulk water diffuses to an NH site. Red asterisks represent exposed amides that are unprotected. Blue asterisks represent "problem cases", where exposed amides are strongly protected. Error bars shown in all panels represent standard deviations.

contacts but side chain interactions, including bifurcated H-bonds. Yet, it is not possible to explain the protection pattern of ubiquitin solely on the basis of H-bonding. Eight strongly protected NH groups remain unaccounted for, as well as nine weakly protected sites (blue and pink, Figure 6b).

Solvent Accessibility. In an effort to rationalize the HDX properties of the remaining sites, we next examined whether a low solvent accessibility might contribute to protection of amide groups that are not H-bonded. NH SASA values range from zero for permanently buried sites all the way to ~10 Å^2 in the disordered C-terminal tail (Figure 5d). It is not unreasonable to assume that SASA values below a certain threshold will slow down HDX by inhibiting NH contact with catalyst and solvent.[11,20−25] Our data offer some clues as to what a suitable threshold might be. D39 is unprotected with SASA = 0.38 Å^2, whereas S20 with SASA = 0.23 Å^2 is protected (Figure 5). This suggests that protection should be a significant factor for SASA values around 0.23 Å^2 and below. When adopting this threshold one can identify I36 and S65 as being occluded from the solvent (in addition to S20). All three residues are protected according to HDX/NMR, despite not being H-bonded (Figure 5). Readers might object to our somewhat heuristic choice of a SASA threshold. Indeed, it will be discussed below that the properties of T9 are not in line with the explanation attempts offered here. Our analysis is nonetheless compatible with the view that the low solvent accessibility of the non-H-bonded residues S20, I36, and S65 is a contributing factor to their experimentally observed protection (Figure 6c).

DOI: 10.1021/acs.biochem.5b00215
Biochemistry 2015, 54, 2683−2692

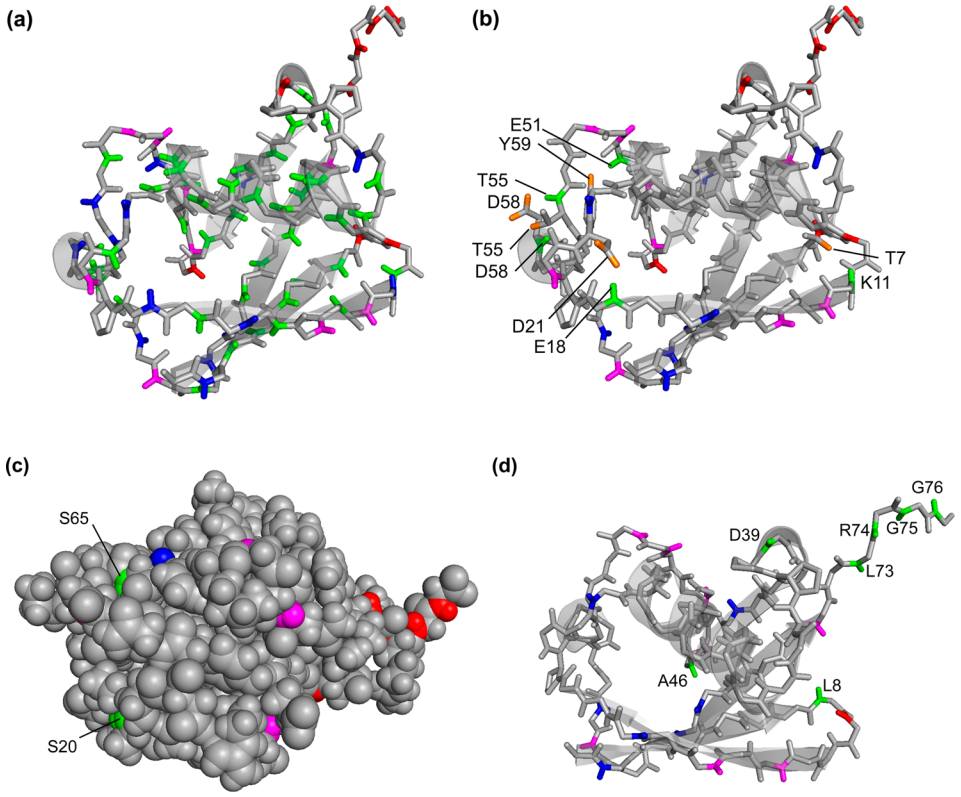

Figure 6. Energy-minimized structure of ubiquitin, where blue/pink/red coloring denotes the level of HDX/NMR protection as in Figure 3. Green represents NH sites with experimental HDX properties that are consistent with features seen in the MD simulations. These "explainable" sites are then grayed out in the subsequent panels. (a) Green: Protected sites that are involved in main chain NH···OC H-bonds. (b) Green: Protected sites that are H-bonded to side chains. Orange: Side chain H-bond acceptors. (c). Green: NH sites protected by low solvent accessibility. I36 is not visible in this all-atom spacefill representation. (d) Green: Unprotected sites that are solvent accessible and not H-bonded.

Unprotected Sites. The above considerations focused on sites that are protected according to HDX/NMR. We attempted to ascribe this protection to H-bonding and NH burial. It is also instructive to pursue the opposite strategy, that is, examine unprotected sites and identify the reason(s) underlying their high HDX rates. From the data compiled in Figure 5, one can identify seven residues that have log *P* values close to zero, with high SASA values and no H-bonding. This group comprises L8, D39, A46, as well as the C-terminal tail (L73−G76). In Figure 6d, the corresponding amides are highlighted in green. These residues conform to the commonly held expectation that a lack of both H-bonding and burial will render NH sites prone to rapid exchange.

Problem Cases. The preceding discussion successfully addressed 79% of the ubiquitin backbone sites. Unfortunately, H-bonding and SASA considerations fail for the remaining 21%. In other words, 15 out of 72 amides do not behave in accordance with classical HDX expectations (Figure 7a). Most of these problem cases are NH groups that show experimental protection, despite having high solvent accessibilities and no H-bonding. This behavior is most dramatically illustrated by Q2, E16, T22, L43, Q62, and T66, which have log *P* values between 2.2 and 3.6. The opposite problem is encountered for T9, where log *P* = 0. This residue is not H-bonded, but it is situated in a narrow pocket with a low SASA value of 0.16 Å^2 (Figure 7b). According to the threshold value identified above these conditions should provide significant protection. For comparison, S20 (SASA = 0.23 Å) exhibits log *P* = 1.6 without H-bonding.

Crystallographically Defined Water Molecules. It has been proposed that H-bonding of exposed amides to crystallographically defined waters can provide HDX protection.[25,33] This proposal envisions that specific solvent molecules are immobilized at the protein surface not only in the crystal, but also in bulk solution.[32] To examine this idea we inspected the X-ray structure of ubiquitin, which comprises 58 crystal waters.[45] Ten of these are H-bonded to exposed NH groups (Figure 7c). Is the presence of these H_2O molecules correlated with HDX protection? Of the six exposed NH sites that exhibit anomalously high protection (Figure 7c, blue), three are H-bonded to crystal water (Q2, E16, and L43); the remaining three are not engaged in defined solvent contacts (T22, Q62, and T66). Focusing on the weakly protected problem cases (Figure 7c, pink), it is seen that four of them (T12, G47, G53, and K63) interact with crystal waters, whereas no water contacts are evident for T14, Q49, D52, and L71. Most importantly, L8, D39, and A46 are H-bonded to crystal waters, despite exhibiting log *P* values close to zero (Figure 7c, gray). This analysis demonstrates a complete lack of correlation between NH protection and H-bonding to crystallographically defined water molecules.

A discussion of NH hydration on the basis of isolated crystal waters may be too simplistic. Some studies suggest that protein surfaces in solution can give rise to H-bonded water cages, resulting in solvent regions that exhibit retarded exchange with the bulk.[63−65] It seems conceivable that such solvent cages might be able to provide HDX protection for exposed amides. To test for the presence of such protecting solvent cages we characterized the water dynamics at the protein surface around

DOI: 10.1021/acs.biochem.5b00215
Biochemistry 2015, 54, 2683−2692

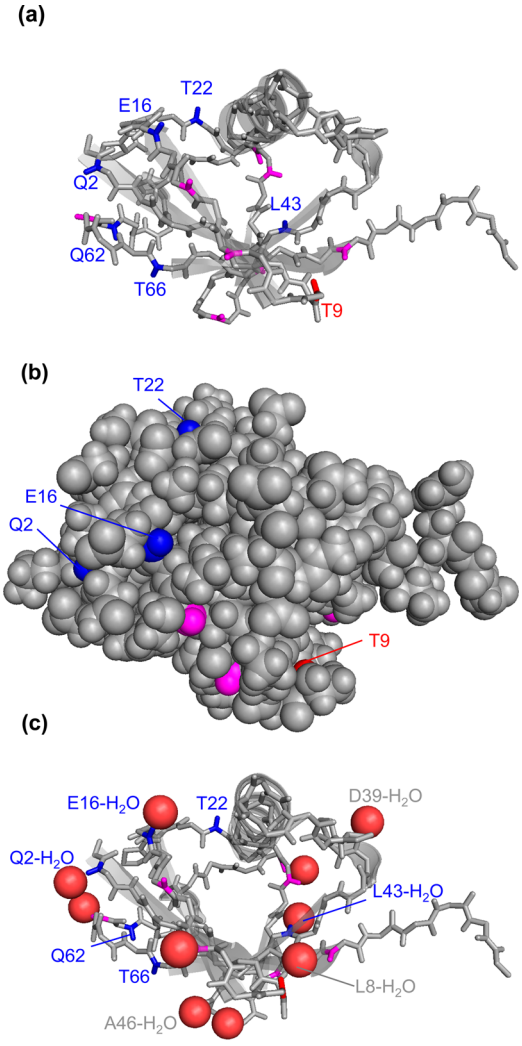

33

Figure 7. (a) Colored NH sites are problem cases, with HDX/NMR properties that are inconsistent with their H-bonding or SASA characteristics. Not all amides are annotated to prevent clutter. (b) Same as in (a), but in all-atom spacefill representation. (c) Ten crystallographically defined waters (red) are H-bonded to backbone amides in the PDB file 1UBQ. Only three out of six strongly protected surface amides interact with water molecules. Highlighted in gray are water-bound surface amides that are unprotected.

each NH site. A "bulk interaction rate" was determined from our MD data, which describes how fast solvent molecules can diffuse from the bulk into the direct vicinity of any given NH. A large interaction rate signifies that solvent molecules adjacent to an NH site are in rapid exchange with the bulk, implying the absence of protecting water networks. The unprotected sites in the C-terminal tail (residues 73−76) provide a reference context for this analysis. Bulk interaction rates for individual amides were generally found to be between 0 and ∼0.05 ps^{-1} (Figure 5e). This range is consistent with earlier reports of surface solvent exchange on picosecond time scales.[65] The key questions is the following: Do exposed NH sites with log $P \gg 0$ exhibit lower bulk interaction rates than NH sites with log $P \approx 0$?

It is most instructive to examine the bulk exchange characteristics of exposed NH sites by focusing on the two extreme cases of strongly protected vs unprotected surface amides (marked with blue and red asterisks, Figure 5e). The average bulk exchange rate of the "blue" sites is 0.020 ± 0.01 ps^{-1}, whereas the "red" sites have a bulk exchange rate of 0.024 ± 0.01 ps^{-1}. The standard deviations of these average rates overlap with each other. While the "red" average is slightly higher, it would be far-fetched to propose that this small differences could be responsible for modulating HDX rates by more than 2 orders of magnitude. We conclude that the solvent interactions for protected and unprotected exposed amides are not significantly different. In other words, our data do not support the idea that the HDX properties of exposed amides can be modulated by partially immobilized water molecules.

Force Fields and Solvent Models. It is unlikely that the lack of correlation between HDX protection and water immobilization in Figure 5e reflects inherent limitations of the MD strategy used here. The data of Figure 5b−e were obtained using the CHARMM22* force field[50] with TIP3P water.[51] Earlier simulations using the same approach were found to be remarkably accurate in folding simulations on a range of proteins.[66] The TIP3P water model has recently been applied to address intricate solvation details at protein surfaces.[64,67] Nonetheless, it is clear that the results of MD simulations can be affected to some extent by the choice of force field.[50,68] To test the robustness of our findings, we repeated the simulations using a different force field (Amber99sb-ILDN[52]) and a different water model (TIP4P[51]). The results obtained in this way are compiled in Supporting Information Figure S1. Comparison of these data with those of Figure 5 shows a very high degree of consistency. These additional data do not affect any of the aforementioned considerations.

CONCLUSIONS

It is sobering that, after 50+ years of using HDX as a structural biology tool,[27] practitioners have now concluded that it is necessary to revisit very simple proteins for conducting "*a detailed hydrogen by hydrogen analysis to examine the bases of structure-rate relationships*".[25] The current work employs all-atom MD simulations in an effort to scrutinize some of the pertinent issues. Computational techniques of the type used here cannot model actual NH → ND conversion events; doing so would require ab initio approaches that are not practical for large systems.[69] Nonetheless, even classical simulations can provide insights that go beyond those obtainable from static crystal structures.[44,66]

It remains undisputed that amides in rigid regions tend to be more protected than those in disordered segments. For ubiquitin, most of the amides in the structured sequence range (residues 1−72) are protected, while the disordered C-terminus (residues 73−76) is unprotected. However, the exact physicochemical features that provide amide NH protection are poorly defined. The results of the current analysis can be summarized as follows (Table 1): (i) H-bonding *always* leads to HDX protection. This includes H-bonds to backbone carbonyls, side chains, as well as bifurcated H-bonds. (ii) For NH sites that are not H-bonded, low SASA values are *often* (but not always) associated with HDX protection. (iii) A lack of H-bonding at solvent-accessible amides does *not* imply that the corresponding sites are unprotected. Instead, many of these amides are characterized by log $P \gg 0$.[25,29−31] Aspect (iii) is the most troublesome finding of our work, as it goes against paradigms that are widely accepted in the HDX community. Most practitioners would concur that log $P \gg 0$ implies either

DOI: 10.1021/acs.biochem.5b00215
Biochemistry 2015, 54, 2683−2692

Table 1. Summary of Backbone NH Protection Behavior

NH structural context	HDX protection status
H-bonded to backbone	protected
H-bonded to side chain	protected
buried (not H-bonded)	often (not always) protected
located in *rigid* region, solvent-accessible, not H-bonded	often (not always) protected
located in *disordered* region, solvent-accessible, not H-bonded	unprotected
H-bonded to crystal water	no effect on protection

H-bonding or NH burial (or both). Our work demonstrates that this view is incorrect for many surface amides. This issue is particularly worrisome for modeling initiatives that rely on HDX data or other "sparse" structural information for elucidating protein conformations.[35,37,42,70] The unexpected HDX behavior displayed by a considerable fraction of amides in a small model protein does not bode well for investigations on larger systems with unknown structures.

Efforts have been undertaken to account for unexpected surface amide protection on the basis of electrostatic factors.[29,30,32] As noted earlier, negative charges in the vicinity of an amide will slow down HDX by raising the NH pK_a.[16−18,71] It remains unclear if such electrostatic effects can be responsible for the surface amide protection considered here. A recent study found no correlation between the HDX rates of surface amides and the calculated electrostatic field.[25] Also, our MD trajectories do not reveal enhanced charge density (from E^- or D^- side chains) in the vicinity of protected surface amides, with the exception of NH sites that engage in bifurcated H-bonds.[60] Electrostatic effects could nonetheless be a contributor to anomalous surface NH protection. Electrostatic modeling approaches require future refinement, as current results are strongly parameter-dependent.[30] Challenges include an adequate description of polarizabilities, dielectric properties, solvent contributions, salt-mediated screening,[18,30] as well as the choice of suitable reference structures.[32]

Our results do not support the proposal[25,33] that crystallographically defined water molecules can protect exposed amides via H-bonding contacts. The validity of this idea had previously been questioned by others.[32] Many of the surface amides in ubiquitin are indeed bound to crystal water, but these interactions are not correlated with the degree of NH protection. We further tested whether protection might arise from higher order water networks. Unfortunately, there is no evidence for differences in the solvation behavior of protected versus unprotected exposed amides. It would be of interest to extend this analysis by including interaction rates of NH sites with OH^- (or OD^-) which acts as HDX catalyst. Regrettably, such calculations require ab initio strategies that are out of reach for systems of the size considered here.[72,73]

The interpretation of HDX kinetics in terms of log P values (eq 3) relies on the adequacy of peptide-calibrated k_{ch} data.[19] This approach has been criticized because peptides may not always properly mimic the environment experienced by protein NH groups (eq 2).[31] Indeed, there are indications of discrepancies between protein and peptide-calibrated data in a few cases.[74,75] Some log P values can also be affected by measurement artifacts. These issues introduce uncertainties, especially for the "weakly protected" sites of Figure 5a. Data obtained for the "strongly protected" and "unprotected" amides are more robust, which is why most of our discussion focused on the latter two categories.

Overall, the results of this study emphasize that HDX data have to be interpreted with caution. Widely accepted tenets such as the putative correlation between HDX protection and amide H-bonding (and/or solvent exclusion) may have to be revised. At the current stage of development, there is no consistent explanation for the fact that surface NH sites can be strongly protected, while structural data show them to reside in a seemingly "open" conformation. These inconsistencies show that the mechanism of protein HDX is far from being understood. Perhaps it is time to move beyond the simple Linderstrøm-Lang formalism (eq 2),[27] which has governed the interpretation of HDX kinetics for decades. Quantum mechanical investigations that take into account the electronic properties of all interaction partners (protein, solvent, catalyst) as well as their conformational dynamics may be required to fully understand the intricacies associated with the seemingly trivial conversion of NH to ND.

■ ASSOCIATED CONTENT

Supporting Information

Figure showing and overview of experimental HDX data, and various properties extracted from a 1 μs Amber99sb-ILDN/TIP4P simulation trajectory. This material is available free of charge via the Internet at http://pubs.acs.org.

■ AUTHOR INFORMATION

Corresponding Author

*E-mail: konerman@uwo.ca.

Funding

Financial support for this work was provided by the Natural Sciences and Engineering Research Council of Canada (NSERC).

Notes

The authors declare no competing financial interest.

■ ACKNOWLEDGMENTS

Some of the simulations for this work were conducted using SHARCNET (www.sharcnet.ca).

■ ABBREVIATIONS

HDX, hydrogen/deuterium (H^1/H^2) exchange; MD, molecular dynamics; NMR, nuclear magnetic resonance; RMSD, root-mean-square deviation; RMSF, root-mean-square fluctuation; SASA, solvent-accessible surface area

■ REFERENCES

(1) Englander, S. W., Mayne, L., and Krishna, M. M. G. (2007) Protein folding and misfolding: Mechanism and principles. *Q. Rev. Biophys. 40*, 287−326.

(2) Fazelinia, H., Xu, M., Cheng, H., and Roder, H. (2014) Ultrafast Hydrogen Exchange Reveals Specific Structural Events during the Initial Stages of Folding of Cytochrome *c*. *J. Am. Chem. Soc. 136*, 733−740.

(3) Ward, M. E., Shi, L., Lake, E., Krishnamurthy, S., Hutchins, H., Brown, L. S., and Ladizhansky, V. (2011) Proton-detected solid-state NMR reveals intramembrane polar networks in a seven-helical transmembrane protein proteorhodopsin. *J. Am. Chem. Soc. 133*, 17434−17443.

(4) Baldwin, R. L. (2011) Early days of protein hydrogen exchange: 1954−1972. *Proteins 79*, 2021−2026.

DOI: 10.1021/acs.biochem.5b00215
Biochemistry 2015, 54, 2683−2692

(5) Pirrone, G. F., Iacob, R. E., and Engen, J. R. (2015) Applications of Hydrogen/Deuterium Exchange MS from 2012 to 2014. *Anal. Chem. 87*, 99−118.
(6) Konermann, L., Pan, J., and Liu, Y. (2011) Hydrogen Exchange Mass Spectrometry for Studying Protein Structure and Dynamics. *Chem. Soc. Rev. 40*, 1224−1234.
(7) Percy, A. J., Rey, M., Burns, K. M., and Schriemer, D. C. (2012) Probing protein interactions with hydrogen/deuterium exchange and mass spectrometry—A review. *Anal. Chim. Acta 721*, 7−21.
(8) Rand, K. D., Zehl, M., Jensen, O. N., and Jørgensen, T. J. D. (2009) Protein Hydrogen Exchange Measured at Single-Residue Resolution by Electron Transfer Dissociation Mass Spectrometry. *Anal. Chem. 81*, 5577−5584.
(9) Marciano, D. P., Dharmarajan, V., and Griffin, P. R. (2014) HDX-MS guided drug discovery: Small molecules and biopharmaceuticals. *Curr. Opin. Struct. Biol.*, 105−111.
(10) Rob, T., Liuni, P., Gill, P. K., Zhu, S. L., Balachandran, N., Berti, P. J., and Wilson, D. J. (2012) Measuring Dynamics in Weakly Structured Regions of Proteins Using Microfluidics-Enabled Subsecond H/D Exchange Mass Spectrometry. *Anal. Chem. 84*, 3771−3779.
(11) Balasubramaniam, D., and Komives, E. A. (2013) Hydrogen-exchangemass spectrometry for the study of intrinsic disorder in proteins. *Biochim. Biophys. Acta 1834*, 1202−1209.
(12) Busenlehner, L. S., Salomonsson, L., Brzezinski, P., and Armstrong, R. N. (2006) Mapping protein dynamics in catalytic intermediates of the redox-driven proton pump cytochrome *c* oxidase. *Proc. Natl. Acad. Sci. U. S. A. 103*, 15398−15403.
(13) Wang, G., Abzalimov, R. R., Bobst, C. E., and Kaltashov, I. A. (2013) Conformer-specific characterization of nonnative protein states using hydrogen exchange and top-down mass spectrometry. *Proc. Natl. Acad. Sci. U. S. A. 110*, 20087−20092.
(14) Keppel, T. R., Howard, B. A., and Weis, D. D. (2011) Mapping Unstructured Regions and Synergistic Folding in Intrinsically Disordered Proteins with Amide H/D Exchange Mass Spectrometry. *Biochemistry 50*, 8722−8732.
(15) Perrin, C. L. (1989) Proton Exchange in Amides: Surprises from Simple Systems. *Acc. Chem. Res. 22*, 268−275.
(16) Fogolari, F., Esposito, G., Viglino, P., Briggs, J. M., and McCammon, J. A. (1998) pK(a) shift effects on backbone amide base-catalyzed hydrogen exchange rates in peptides. *J. Am. Chem. Soc. 120*, 3735−3738.
(17) Molday, R. S., Englander, S. W., and Kallen, R. G. (1972) Primary Structure Effects on Peptide Hydrogen Exchange. *Biochemistry 11*, 150−158.
(18) Abdolvahabi, A., Gober, J. L., Mowery, R. A., Shi, Y. H., and Shaw, B. F. (2014) Metal-Ion-Specific Screening of Charge Effects in Protein Amide H/D Exchange and the Hofmeister Series. *Anal. Chem. 86*, 10303−10310.
(19) Bai, Y., Milne, J. S., Mayne, L., and Englander, S. W. (1993) Primary Structure Effects on Peptide Group Hydrogen Exchange. *Proteins: Struct., Funct., Genet. 17*, 75−86.
(20) Fajer, P. G., Bou-Assaf, G. M., and Marshall, A. G. (2012) Improved Sequence Resolution by Global Analysis of Overlapped Peptides in Hydrogen/Deuterium Exchange Mass Spectrometry. *J. Am. Soc. Mass Spectrom. 23*, 1202−1208.
(21) Yan, X., Pérez, E., Leid, M., Schimerlik, M. I., de Lera, A. R., and Deinzer, M. L. (2007) Deuterium exchange and mass spectrometry reveal the interaction differences of two synthetic modulators of RXRαLBD. *Protein Sci. 16*, 2491−2501.
(22) Hughson, F. M., Wright, P. E., and Baldwin, R. L. (1990) Structural Characterisation of a Partly Folded Apomyoglobin Intermediate. *Science 249*, 1544−1548.
(23) Sperry, J. B., Smith, C. L., Caparon, M. G., Ellenberger, T., and Gross, M. L. (2011) Mapping the Protein−Protein Interface between a Toxin and Its Cognate Antitoxin from the Bacterial Pathogen Streptococcus pyogenes. *Biochemistry 50*, 4038−4045.
(24) Shan, Y., Arkhipov, A., Kim, E. T., Pan, A. C., and Shaw, D. E. (2013) Transitions to catalytically inactive conformations in EGFR kinase. *Proc. Natl. Acad. Sci. U. S. A. 110*, 7270−7275.
(25) Skinner, J. J., Lim, W. K., Bedard, S., Black, B. E., and Englander, S. W. (2012) Protein hydrogen exchange: Testing current models. *Protein Sci. 21*, 987−995.
(26) Pan, Y., and Briggs, M. S. (1992) Hydrogen Exchange in Native and Alcohol Forms of Ubiquitin. *Biochemistry 31*, 11405−11412.
(27) Hvidt, A., and Nielsen, S. O. (1966) Hydrogen exchange in proteins. *Adv. Protein Chem. 21*, 287−386.
(28) Sowole, M. A., Alexopoulos, J. A., Cheng, Y.-Q., Ortega, J., and Konermann, L. (2013) Activation of ClpP Protease by ADEP Antibiotics: Insights from Hydrogen Exchange Mass Spectrometry. *J. Mol. Biol. 425*, 4508−4519.
(29) Anderson, J. S., Hernandez, G., and LeMaster, D. M. (2008) A billion-fold range in acidity for the solvent-exposed amides of Pyrococcus furiosus rubredoxin. *Biochemistry 47*, 6178−6188.
(30) Hernandez, G., Anderson, J. S., and LeMaster, D. M. (2009) Polarization and Polarizability Assessed by Protein Amide Acidity. *Biochemistry 48*, 6482−6494.
(31) Li, R., and Woodward, C. (1999) The hydrogen exchange core and protein folding. *Protein Sci. 8*, 1571−1590.
(32) Anderson, J. S., Hernandez, G., and LeMaster, D. M. (2013) Assessing the chemical accuracy of protein structures via peptide acidity. *Biophys. Chem. 171*, 63−75.
(33) Skinner, J. J., Lim, W. K., Bédard, S., Black, B. E., and Englander, S. W. (2012) Protein dynamics viewed by hydrogen exchange. *Protein Sci. 21*, 996−1005.
(34) Alexopoulos, J. A., Guarnéa, A., and Ortega, J. (2012) ClpP: A structurally dynamic protease regulated by AAA+ proteins. *J. Struct. Biol. 179*, 202−210.
(35) Gsponer, J., Hopearuoho, H., Whittaker, S. B. M., Spence, G. R., Moore, G. R., Paci, E., Radford, S. E., and Vendruscolo, M. (2006) Determination of an ensemble of structures representing the intermediate state of the bacterial immunity protein Im7. *Proc. Natl. Acad. Sci. U. S. A. 103*, 99−104.
(36) Craig, P. O., Lätzer, J., Weinkam, P., Hoffman, R. M. B., Ferreiro, D. U., Komives, E. A., and Wolynes, P. G. (2011) Prediction of native-state hydrogen exchange from perfectly funneled energy landscapes. *J. Am. Chem. Soc. 133*, 17463−17472.
(37) Sheinerman, F. B., and Brooks, C. L., III. (1998) Molecular picture of folding of a small α/β protein. *Proc. Natl. Acad. Sci. U. S. A. 95*, 1562−1567.
(38) Garcia, A. E., and Hummer, G. (1999) Conformational dynamics of cytochrome c: Correlation to hydrogen exchange. *Proteins 36*, 175−191.
(39) Petruk, A. A., Defelipe, L. A., Limardo, R. G. R., Bucci, H., Marti, M. A., and Turjanski, A. G. (2013) Molecular Dynamics Simulations Provide Atomistic Insight into Hydrogen Exchange Mass Spectrometry Experiments. *J. Chem. Theory Comput. 9*, 658−669.
(40) Hsu, Y. H., Bucher, D., Cao, J., Li, S., Yang, S. W., Kokotos, G., Woods, V. L., McCammon, J. A., and Dennis, E. A. (2013) Fluoroketone Inhibition of Ca^{2+}-Independent Phospholipase A(2) through Binding Pocket Association Defined by Hydrogen/Deuterium Exchange and Molecular Dynamics. *J. Am. Chem. Soc. 135*, 1330−1337.
(41) Xu, J., Lee, Y. J., Beamer, L. J., and Van Doren, S. R. (2015) Phosphorylation in the Catalytic Cleft Stabilizes and Attracts Domains of a Phosphohexomutase. *Biophys. J. 108*, 235−337.
(42) Liu, T., Pantazatos, D., Li, S., Hamuro, Y., Hilser, V. J., and Woods, V. L. (2012) Quantitative assessment of protein structural models by comparison of H/D exchange MS data with exchange behavior accurately predicted by DXCOREX. *J. Am. Soc. Mass Spectrom. 23*, 43−56.
(43) Bahar, I., Wallqvist, A., Covell, D. G., and Jernigan, R. L. (1998) Correlation between Native-State Hydrogen Exchange and Cooperative Residue Fluctuations from a Simple Model. *Biochemistry 37*, 1067−1075.

DOI: 10.1021/acs.biochem.5b00215
Biochemistry 2015, 54, 2683−2692

(44) Piana, S., Lindorff-Larsen, K., and Shaw, D. E. (2013) Atomic-level description of ubiquitin folding. *Proc. Natl. Acad. Sci. U. S. A. 110*, 5915−5920.
(45) Vijay-Kumar, S., Bugg, C. E., and Cook, W. J. (1987) Structure of Ubiquitin Refined at 1.8 A Resolution. *J. Mol. Biol. 194*, 531−544.
(46) Bougault, C., Feng, L. M., Glushka, J., Kupce, E., and Prestegard, J. H. (2004) Quantitation of rapid proton-deuteron amide exchange using hadamard spectroscopy. *J. Biomol. NMR 28*, 385−390.
(47) Johnson, E. C., Lazar, G. A., Desjarlais, J. R., and Handel, T. M. (1999) Solution structure and dynamics of a designed hydrophobic core variant of ubiquitin. *Struct. Folding Des. 7*, 967−976.
(48) Hess, B., Kutzner, C., van der Spoel, D., and Lindahl, E. (2008) GROMACS 4: Algorithms for Highly Efficient, Load-Balanced, and Scalable Molecular Simulation. *J. Chem. Theory Comput. 4*, 435−447.
(49) Berendsen, H. J., van der Spoel, D., and van Drunen, R. (1995) GROMACS: A message-passing parallel molecular dynamics implementation. *Comput. Phys. Commun. 91*, 43−56.
(50) Piana, S., Lindorff-Larsen, K., and Shaw, D. E. (2011) How Robust Are Protein Folding Simulations with Respect to Force Field Parameterization? *Biophys. J. 100*, L47−L49.
(51) Jorgensen, W. L., Chandrasekhar, J., Madura, J. D., Impey, R. W., and Klein, M. L. (1983) Comparison of simple potential functions for simulating liquid water. *J. Chem. Phys. 79*, 926−935.
(52) Lindorff-Larsen, K., Piana, S., Palmo, K., Maragakis, P., Klepeis, J. L., Dror, R. O., and Shaw, D. E. (2010) Improved side-chain torsion potentials for the Amber ff99SB protein force field. *Proteins 78*, 1950−1958.
(53) Cisneros, G. A., Karttunen, M., Ren, P. Y., and Sagui, C. (2014) Classical Electrostatics for Biomolecular Simulations. *Chem. Rev. 114*, 779−814.
(54) Goyal, P., Qian, H. J., Irle, S., Lu, X. Y., Roston, D., Mori, T., Elstner, M., and Cui, Q. (2014) Molecular Simulation of Water and Hydration Effects in Different Environments: Challenges and Developments for DFTB Based Models. *J. Phys. Chem. B 118*, 11007−11027.
(55) Bussi, G., Donadio, D., and Parrinello, M. (2007) Canonical sampling through velocity rescaling. *J. Chem. Phys. 126*, 0141011−0141017.
(56) Berendsen, H. J. C., Postma, J. P. M., Vangunsteren, W. F., Dinola, A., and Haak, J. R. (1984) Molecular dynamics with coupling to an external bath. *J. Chem. Phys. 81*, 3684−3690.
(57) Hess, B., Henk, B., Berendsen, H. J. C., and Fraaije, J. G. E. M. (1997) LINCS: A linear constraint solver for molecular simulations. *J. Comput. Chem. 18*, 1463−1472.
(58) Miyamoto, S., and Kollman, P. A. (1992) SETTLE: An Analytical Version of the SHAKE and RATTLE Algorithm for Rigid Water Models. *J. Comput. Chem. 13*, 952−962.
(59) Essmann, U., Perera, L., Berkowitz, M. L., Darden, T., Lee, H., and Pedersen, L. G. (1995) A Smooth Particle Mesh Ewald Method. *J. Chem. Phys. 103*, 8577−8593.
(60) Torshin, I. Y., Weber, I. T., and Harrison, R. W. (2002) Geometric criteria of hydrogen bonds in proteins and identification of 'bifurcated' hydrogen bonds. *Protein Eng. 15*, 359−363.
(61) Eisenhaber, F., Lijnzaad, P., Argos, P., Sander, C., and Scharf, M. (1995) The double cubic lattice method: Efficient approaches to numerical integration of surface area and volume and to dot surface contouring of molecular assemblies. *J. Comput. Chem. 16*, 273−284.
(62) Li, A. J., and Nussinov, R. (1998) A set of van der Waals and Coulombic radii of protein atoms for molecular and solvent-accessible surface calculation, packing evaluation, and docking. *Proteins 32*, 111−127.
(63) Mallajosyula, S. S., Vanommeslaeghe, K., and MacKerell, A. D. (2014) Perturbation of Long-Range Water Dynamics as the Mechanism for the Antifreeze Activity of Antifreeze Glycoprotein. *J. Phys. Chem. B 118*, 11696−11706.
(64) Nibali, V. C., and Havenith, M. (2014) New Insights into the Role of Water in Biological Function: Studying Solvated Biomolecules Using Terahertz Absorption Spectroscopy in Conjunction with Molecular Dynamics Simulations. *J. Am. Chem. Soc. 136*, 12800−12807.
(65) Krishnamoorthy, A. N., Holm, C., and Smiatek, J. (2014) Local Water Dynamics around Antifreeze Protein Residues in the Presence of Osmolytes: The Importance of Hydroxyl and Disaccharide Groups. *J. Phys. Chem. B 118*, 11613−11621.
(66) Lindorff-Larsen, K., Piana, S., Dror, R. O., and Shaw, D. E. (2011) How Fast-Folding Proteins Fold. *Science 334*, 517−520.
(67) Martin, D. R., and Matyushov, D. V. (2015) Dipolar Nanodomains in Protein Hydration Shells. *J. Phys. Chem. Lett. 6*, 407−412.
(68) Cino, E. A., Choy, W. Y., and Karttunen, M. (2012) Comparison of Secondary Structure Formation Using 10 Different Force Fields in Microsecond Molecular Dynamics Simulations. *J. Chem. Theory Comput. 8*, 2725−2740.
(69) Ijaz, W., Gregg, Z., and Barnes, G. L. (2013) Complex Formation during SID and Its Effect on Proton Mobility. *J. Phys. Chem. Lett. 4*, 3935−3939.
(70) Moult, J., Fidelis, K., Kryshtafovych, A., Schwede, T., and Tramontano, A. (2014) Critical assessment of methods of protein structure prediction (CASP) - round x. *Proteins 82*, 1−6.
(71) Shaw, B. F., Arthanari, H., Narovlyansky, M., Durazo, A., Frueh, D. P., Pollastri, M. P., Lee, A., Bilgicer, B., Gygi, S. P., Wagner, G., and Whitesides, G. M. (2010) Neutralizing Positive Charges at the Surface of a Protein Lowers Its Rate of Amide Hydrogen Exchange without Altering Its Structure or Increasing Its Thermostability. *J. Am. Chem. Soc. 132*, 17411−17425.
(72) Tuckerman, M. E., Marx, D., and Parrinello, M. (2002) The nature and transport mechanism of hydrated hydroxide ions in aqueous solution. *Nature 417*, 925−929.
(73) Crespo, Y., and Hassanali, A. (2015) Unveiling the Janus-Like Properties of OH. *J. Phys. Chem. Lett. 6*, 272−278.
(74) Rand, K. D., and Jørgensen, T. J. D. (2007) Development of a Peptide Probe for the Occurrence of Hydrogen (^{1}H/^{2}H) Scrambling upon Gas-Phase Fragmentation. *Anal. Chem. 79*, 8686−8693.
(75) Del Mar, C., Greenbaum, E. A., Mayne, L., Englander, S. W., and Woods, V. L. (2005) Structure and properties of α-synuclein and other amyloids determined at the amino acid level. *Proc. Natl. Acad. Sci. U. S. A. 102*, 15477−15482.

DOI: 10.1021/acs.biochem.5b00215
Biochemistry 2015, 54, 2683−2692